Laskey, R. A., & Mills, A. D. (1975) *Eur. J. Biochem. 56*, 335-341.
Libby, P. R. (1978) *J. Biol. Chem. 253*, 233-237.
Lowry, O. H., Rosebrough, J. N., Farr, A. L., & Randall, R. J. (1951) *J. Biol. Chem. 193*, 265-275.
Lue, P. F., Gornall, A. G., & Liew, C. C. (1973) *Can. J. Biochem. 51*, 1177-1194.
Nohara, H., Takahashi, T., & Ogata, K. (1968) *Biochim. Biophys. Acta 154*, 529-539.
Noland, J., Hardin, J. M., & Shepherd, G. R. (1971) *Biochim. Biophys. Acta 246*, 263-268.
Sures, I., & Gallwitz, D. (1975) *FEBS Lett. 53*, 92-94.
Thwaits, B. H., Brandt, W. F., & von Holt, C. (1976a) *FEBS Lett. 71*, 193-196.
Thwaits, B. H., Brandt, W. F., & von Holt, C. (1976b) *FEBS Lett. 71*, 197-199.
Vidali, G., Boffa, L. C., & Allfrey, V. G. (1972) *J. Biol. Chem. 247*, 7365-7373.

Equilibrium Substrate Binding Studies of the Malic Enzyme of Pigeon Liver. Equivalence of Nucleotide Sites and Anticooperativity Associated with the Binding of L-Malate to the Enzyme-Manganese(II)-Reduced Nicotinamide Adenine Dinucleotide Phosphate Ternary Complex†

Terry A. Pry‡ and Robert Y. Hsu*

ABSTRACT: Malic enzyme (ME) from pigeon liver is a tetrameric protein containing apparently identical subunits. In the present study, equilibrium dialysis and fluorescence titration techniques are employed to determine the binding parameters of nucleotide cofactors, malate, and the inhibitor oxalate. ME binds $NADP^+$ or NADPH at four independent and equivalent sites with dissociation constants of 1.33 μM (pH 7.5, 4 °C) and 0.29 μM (pH 7.0, 5 °C), respectively, showing "all-of-the-sites" reactivity. The affinity of both nucleotides decreases with increasing temperature, yielding $\Delta H_{dissociation}$ values of 11.4 kcal/mol for E-$NADP^+$ and 8.9 kcal/mol for E-NADPH, thus implicating the involvement of polar forces in the binding process. The affinity of $NADP^+$ is independent of pH between 6.1 and 8.4, whereas that of NADPH is highly pH dependent and decreases ~63-fold from pH 6.0 to pH 8.0. The pH profile suggests the participation of a protonated enzyme group(s) (pK = 7.2-7.5) in NADPH binding, probably a histidine residue. The affinity of $NADP^+$ is enhanced ca. twofold by pyruvate, in the presence of Mn^{2+} (50-100 μM) saturating only two "tight" metal sites [Hsu, R. Y., Mildvan, A. S., Chang, G. G., & Fung, C. H. (1976) *J. Biol. Chem. 251*, 6574]. Binding of Mn^{2+} at weak metal sites ($K_D \simeq 0.9$ mM) prevents this change. Malate binds free ME or binary E-Mn^{2+} and E-$NADP^+$ (H) complexes weakly with dissociation constants of ≥2 mM. The affinity is significantly increased by Mn^{2+} and NADPH in the ternary E-Mn^{2+}-NADPH complex, yielding two "tight" (K_D = 22-30 μM) and two "weak" (K_D = 250-400 μM) malate sites per enzyme tetramer as the result of either preexisting nonidentity or negative cooperativity between initially identical sites. The transition-state inhibitor oxalate binds ME tightly (K_D = 65 μM) at the two tight malate sites, showing "half-of-the-sites" stoichiometry. The binding parameters are unaffected by Mn^{2+}, whereas the affinity of this inhibitor is enhanced 3.5-fold by saturation with NADPH. Further evidence for the half-of-the-sites reactivity of the affinity label bromopyruvate [Pry, T. A., & Hsu, R. Y. (1978) *Biochemistry 17*, 4024] is obtained by sequential modification of the four putatively identical SH groups of ME with bromopyruvate, 5,5′-dithiobis(2-nitrobenzoic acid), and $K^{14}CN$. The modified enzyme has a structure of $E_4(S\text{-pyr})_2(S\text{-}^{14}CN)_2$ and is "inactive" in the reaction with malate. In contrast, the $E(S\text{-}^{14}CN)_4$ derivative prepared in the absence of bromopyruvate is completely active. The oxidative decarboxylase reaction is inhibited by high concentrations (≥0.3 mM) of malate in the presence of tightly bound Mn^{2+}. Direct binding studies show a parallel increase in the affinity of NADPH, confirming our previous notion [Reynolds, C. H., Hsu, R. Y., Matthews, B., Pry, T. A., & Dalziel, K. (1978) *Arch. Biochem. Biophys. 189*, 309] that malate inhibits the rate-limiting NADPH release step.

Pigeon liver malic enzyme [L-malate:$NADP^+$ oxidoreductase (decarboxylating), EC 1.1.1.40] is a tetramer composed of identical or nearly identical subunits (Nevaldine et al., 1974). The substrates $NADP^+$ and malate exhibit typical Michaelis-Menten (i.e., noncooperative) kinetic behavior in the oxidative decarboxylase reaction at a constant level of Mg^{2+} (Hsu et al., 1967). The initial velocity and product inhibition patterns are consistent with a sequential, ordered kinetic mechanism with $NADP^+$ adding first, followed by malate, and the release of CO_2, pyruvate, and NADPH as products. More recently, the possibility of anticooperativity or nonidentical active sites is suggested by the following observations: (a) metal binding studies indicating the presence of two "tight" and two to four "weak" Mn^{2+} sites per enzyme tetramer (Hsu et al., 1976); (b) the apparent kinetic negative cooperativity of Mn^{2+}, potentiated by the substrate malate (Hsu et al., 1976); (c) a transient burst of enzyme-bound NADPH which equals approximately half of the active-site concentration

† From the Department of Biochemistry, State University of New York, Upstate Medical Center, Syracuse, New York 13210. *Received August 9, 1979.* Supported in part by grants from the National Institutes of Health (AM 13390 and 5507RR05402). This research is derived from the dissertation of T.A.P. presented in partial fulfillment for the requirements of a Ph.D. degree.
‡ Present address: Lipid Metabolism Laboratory, Veteran's Administration Hospital, Madison, WI 53705.

0006-2960/80/0419-0951$01.00/0

(Reynolds et al., 1978b); (d) the "half-of-the-sites" reactivity of bromopyruvate which inactivates the enzyme after alkylating two of the four "essential" SH groups (Chang & Hsu, 1977a). The unmodified SH groups react with nonspecific reagents such as *N*-ethylmaleimide and 5,5′-dithiobis(2-nitrobenzoic acid) more slowly than do the SH groups of the native enzyme (Pry & Hsu, 1978).

The present work is undertaken to determine the substrate binding parameters of this enzyme in an attempt to uncover further evidence for anticooperative behavior. A preliminary report showing biphasic binding of malate and half-of-the-sites binding of the inhibitor oxalate has been published (Pry, 1979). A steady-state kinetic analysis is carried out in the following paper (Hsu & Pry, 1980) to evaluate the functional significance of heterogeneity in Mn^{2+} and malate binding sites.

Experimental Section

Materials

TEA-HCl (A grade),[1] EDTA, Tris-HCl (enzyme grade), DTT, bromopyruvate, and DTNB (Calbiochem), L-malic acid (Schwarz/Mann), $NADP^+$ and NADPH (P-L Biochemicals), Sephadex G-10 and Sephadex G-200 (Pharmacia), Dowex 1-X10 (Mallinckrodt), DE-52 (Whatman), [U-^{14}C]-L-malate and [^{14}C]$NADP^+$ (carbonyl) (Amersham), Aquasol, [U-^{14}C]oxalate, and K^{14}CN (New England Nuclear), and $MnCl_2$ (Fischer Scientific) were purchased from the above sources. Distilled, deionized water was used throughout this work. The nucleotide solutions were made up fresh daily. The concentration of NADPH was determined spectrophotometrically with the use of a molar extinction coefficient of 6.2×10^3 at 340 nm.

Methods

Pigeon liver malic enzyme was purified according to Hsu & Lardy (1967a). Typical yields of 100–170 mg of purified malic enzyme were obtained from 450 to 500 g of pigeon livers. Highly active preparations (sp act. 39–42 units/mg) showing homogeneity in the analytical ultracentrifuge were used. The purified enzyme was dialyzed exhaustively against 50 mM Tris-HCl buffer, pH 7.0, containing 5 mM DTT, 0.1 mM EDTA, and 10% glycerol and stored at −20 °C. The dialyzed enzyme solution was stable at this temperature for several months. Prior to each use, the enzyme was thawed and dialyzed against the appropriate TEA-HCl buffers (containing DTT and in some cases also EDTA) indicated for the individual experiments. Protein concentration was determined with a Gilford 2000 spectrophotometer at 278 nm with an extinction coefficient of 0.86 for a 0.1% w/v protein solution (Hsu & Lardy, 1967a). A tetrameric molecular weight of 260 000 and a subunit molecular weight of 65 000 were used in all calculations (Nevaldine et al., 1974).

Enzyme Assays. Oxidative decarboxylase activity was assayed according to Hsu & Lardy (1967a). The formation of NADPH was monitored at 340 nm in either a Cary Model 16 spectrophotometer equipped with a Hewlett-Packard 17500A recorder or a Gilford Model 250 spectrophotometer equipped with a Gilford 6051 recorder. The cell compartment was thermostated at 30 °C with a Haake FS constant-temperature bath. All reagents were brought to 30 °C before mixing. The reaction mixture consisted of TEA-HCl buffer (pH 7.4), 200 μmol, sodium L-malate (Schwarz/Mann), pH 7.4, 1.5 μmol, $MnCl_2$, 12 μmol, $NADP^+$, 0.63 μmol, and an appropriate amount of enzyme in a total volume of 3.0 mL. Enzyme was added to start the reaction. The formation of NADPH was always linear with time. One unit of enzyme is defined as the amount which catalyzes the conversion of 1 μmol of substrate per minute under the conditions of the assay. Specific activity is expressed as units per milligram of protein. The kinetic assays were performed essentially as described above except that the reactions were carried out at pH 7.0 in TEA-HCl buffer, 150 μmol; the $MnCl_2$ additions were from 0.03 to 90 μmol and the malate additions were from 0.015 to 45 μmol.

Purification of Radioactive Ligands. Commercially obtained carbonyl-labeled [^{14}C]$NADP^+$, [U-^{14}C]-L-malate, and [U-^{14}C]oxalate were purified through chromatographic procedures and stored at −20 °C as lyophilized powders before use. K^{14}CN was used without purification. The radioisotope specific activity (cpm/micromole of ligand) was calculated from measurements of ligand concentration, and the radioactivity was determined from a sample counted in the Beckman LS-150 scintillation counter.

[^{14}C]$NADP^+$ was purified by the procedure of Winer (1964) through a DE-52 column (1.5 × 3.0 cm) with a linear gradient of 10 mM Tris-HCl, pH 7.5 (100 mL), to 10 mM Tris-HCl and 0.5 M NaCl, pH 7.5 (100 mL). The nucleotide peak (as measured by absorption at 258 nm) was then lyophilized, dissolved in water, desalted through a Sephadex G-10 column (1.4 × 75 cm) with water, and stored at −20 °C as a lyophilized powder. The concentration of $NADP^+$ was assayed by using malic enzyme with the nucleotide as the limiting substrate. [^{14}C]-L-Malate was purified through a Dowex 1-X10 column (1.5 × 8 cm) with a linear gradient of 0–50 mM HCl (100 mL total volume). Malate was neutralized with 5 M K_2CO_3 prior to chromatography. The effluent which contained [^{14}C]malate was subjected to successive lyophilization to remove HCl and stored as before after determination of its concentration (by malic enzyme) and radioactivity. [^{14}C]Oxalate was purified similarly (Owens et al., 1953) on a 1.5 × 10 cm Dowex 1-X10 column and eluted with a linear gradient of 0–1 N HCl (100 mL total volume). After lyophilization to remove HCl, the concentration of oxalate was determined colorimetrically (Lewis & Weinhouse, 1957) by titrating (at 60 °C) a sample of this compound in mineral oil, which had been acidified with H_2SO_4, with 0.1 N potassium permanganate to a permanent pink.

Equilibrium Dialysis Studies. Binding measurements were made with an eight-cell equilibrium dialysis apparatus (Bel-Art) which required a minimum volume of only 60 μL of solution per chamber in each cell. Glycerol was removed from malic enzyme by dialysis against 50 mM TEA-HCl buffer, containing 1 mM DTT and 0.1 mM EDTA (malate studies only), at the appropriate pH described for each equilibrium dialysis experiment. The equilibrium dialysis membrane was obtained from dialysis tubing (VWR Scientific, 0.75-in. diameter) which had been boiled for 5 min in 50 mM EDTA and 5% Na_2CO_3 (pH 7.0) and stretched to increase porosity. The stretched membrane was stored in 50% ethanol (Craig & King, 1962). Before each use, the membrane was soaked for 12 h in the dialysis buffer described above, blotted to remove excess liquid, and placed between the two halves of the equilibrium dialysis apparatus. A 1-mm glass bead was placed in each chamber to aid in stirring, and the two halves of the apparatus were then joined firmly with bolts and sealed

[1] Abbreviations used: TEA-HCl, triethanolamine hydrochloride; Tris, tris(hydroxymethyl)aminomethane; EDTA, ethylenediaminetetraacetic acid; DTT, dithiothreitol; DE-52, diethylaminoethylcellulose 52; DTNB, 5,5′-dithiobis(2-nitrobenzoic acid); TNB, 5-thio(2-nitrobenzoic acid); NEM, *N*-ethylmaleimide; Oxa, oxalate; Mal, L-malate.

with Teflon tape. Aliquots of buffer and ligand(s) were added to both chambers whereas malic enzyme was added to a single chamber. The final volumes in each pair of sample chambers were equal and constant for each experiment but ranged from 60 to 80 μL between experiments. The protein concentrations and range of radioactive ligand concentrations used in these experiments are described in the figure legends. Control studies indicated that equilibration between opposite chambers was obtained in less than 2 h at the temperatures (4–26 °C) employed; however, the entire apparatus was always rotated (~30 rpm) for 4–5 h to ensure complete equilibration. After equilibration, the content of each sample chamber was removed. Aliquots (5–50 μL) were then transferred by a micropipet to scintillation vials containing 15 mL of Aquasol and counted in a Beckman LS-150 scintillation counter. The radioactivity in the chamber lacking malic enzyme was taken as a measure of the free (unbound) ligand. The concentration of bound ligand was determined from the difference in radioactivity between each pair of opposite chambers. A portion of protein was routinely assayed for oxidative decarboxylase activity and protein concentration at the start and conclusion of each experiment. There was no significant change in either measurement, indicating that the enzyme was stable during the course of equilibration and that there was no significant dilution by osmosis. Control studies also indicated that there was no protein leakage through the stretched dialysis membrane over a 5-h period at either 4 or 26 °C.

Fluorescence Studies. Fluorescence titrations were carried out with an Aminco-Bowman spectrofluorometer equipped with a thermojacketed cuvette holder and a rectangular micro quartz cell (0.5 × 0.5 cm). Temperature was controlled with a Hetofrig constant-temperature circulator. For low-temperature studies (4 °C), dry nitrogen was passed through the cuvette chamber to minimize condensation.

NADPH fluorescence titrations were performed essentially according to Hsu & Lardy (1967b). Successive aliquots (2–5 μL) of NADPH (60–200 μM) were added on a glass spatula to cuvettes containing 0.2 to 0.3 mL of 50 mM TEA-HCl buffer, in the absence or presence of malic enzyme. Formation of the binary enzyme–nucleotide complex results in a large enhancement of nucleotide fluorescence which was monitored at an excitation wavelength of 350 nm and emission wavelength of 470 nm. The fluorescence yield of this complex was further enhanced by malate in the presence of Mn^{2+} and this enhancement was used to quantitate malate binding. In these experiments, the titrations were carried out by the addition of malate to cuvettes containing enzyme, $MnCl_2$, and an amount of NADPH which saturated the available nucleotide binding sites. Control studies have shown that malate does not affect the fluorescence of free (unbound) NADPH.

The fluorescence increment obtained upon addition of a ligand to an enzyme solution is the sum of the fluorescence of the free and bound ligand as given by the equation (Adelstein, 1965; Winer et al., 1959)

$$F = \beta[L]_f + \beta'[EL] \quad (1)$$

Also

$$K_D = [E]_f[L]_f/[EL] \quad (2)$$

where F is the fluorescence value after correcting for volume dilution. $[L]_f$ and $[EL]$ are the concentrations (in μM) of free and bound ligand, and β and β' are the micromolar fluorescence emittence of each, in arbitrary units. In titration experiments with NADPH, these values refer to those obtained with free and enzyme-bound NADPH in the binary complex, respectively, whereas, in titration experiments with malate, $\beta = 0$ and β' refers to the incremental increase of NADPH fluorescence in the E–Mn^{2+}–NADPH complex upon binding of malate. K_D is the dissociation constant of the EL complex.

For NADPH titrations, β may be determined directly from the linear titration plot of NADPH without enzyme. β' was determined from the initial slope of an F vs. [NADPH] plot at high enzyme concentration where $[E]_t > K_D \gg [L]_t$. $[E]_t$ and $[L]_t$ are, respectively, the total enzyme and ligand concentrations, and $[E]_t = [E]_f + [EL]$.

The affinity of malate was much lower, however, which necessitated the evaluation of β' for malate by a method essentially according to that described by Tomkins et al. (1962) and Fromm (1963). Malate titrations were performed at several enzyme concentrations from which the initial slopes of $F/[L]_t$ were plotted in a double-reciprocal plot against $[E]_t$. β' for malate was then calculated from the reciprocal of the vertical intercept obtained by extrapolation of the plot to infinite enzyme concentration.

The concentrations of free and bound ligand were determined as follows. Since

$$[L]_t = [L]_f + [EL] \quad (3)$$

substitution into eq 1 obtains

$$[EL] = \frac{F - \beta[L]_t}{\beta' - \beta} \quad (4)$$

$[L]_f$ was then obtained from eq 3. For malate titrations, $\beta = 0$ and eq 4 reduces to $[EL] = F/\beta'$.

Data Analysis. The binding parameters of either $NADP^+$, NADPH, or oxalate with malic enzyme were calculated according to Scatchard (1949), based upon a single class of equivalent and noninteracting binding sites:

$$\frac{\bar{v}}{[L]_f} = \frac{-\bar{v}}{K_D} + \frac{n}{K_D} \quad (5)$$

$\bar{v}$ is the experimentally determined number of bound ligand and n is the number of ligand binding sites per enzyme tetramer. K_D and n were obtained from a plot of $\bar{v}/[L]_f$ vs. $\bar{v}$. In these plots, the points were experimental observations and the lines were drawn by regression analysis.

Nonlinear Scatchard plots obtained in malate binding studies were fitted to a simple case of two sets of binding sites with different affinities (Edsall & Wyman, 1958):

$$\bar{v} = \frac{[L]_f n}{K_D + [L]_f} + \frac{[L]_f n'}{K_D' + [L]_f} \quad (6)$$

K_D and n are the dissociation constant and stoichiometry, respectively, for the first class of malate binding sites whereas K_D' and n' represent those values for the second class of malate sites. Rough estimates of these parameters were obtained from visual inspection of the Scatchard plot. These values were refined by a method of reiterative approximations (Weder et al., 1974), until the deviation of experimental points from the calculated curve (solid lines in Figure 5) was at a minimum.

Alternatively, ligand dissociation constants in fluorescence titration experiments were estimated from the horizontal intercepts of double-reciprocal replots of $1/\Delta F$ vs. $1/[L]_f$ according to Adelstein (1965)

$$\frac{(\beta' - \beta)[E]_t}{\Delta F} = \frac{K_D}{[L]_f} + 1 \quad (7)$$

where ΔF represents the difference between the observed fluorescence intensity (F) and the fluorescence intensity of the ligand in free form (without enzyme) and equals $[EL](\beta' - \beta)$.

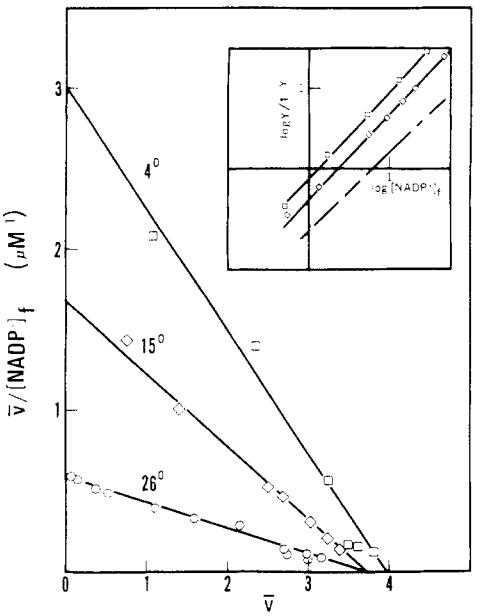

FIGURE 1: Equilibrium binding of $NADP^+$ and the effect of temperature on its binding parameters. The $NADP^+$ binding studies were performed by the equilibrium dialysis technique as described under Methods. Both chambers of each dialysis cell contained 50 mM TEA-HCl buffer, pH 7.5, 1 mM DTT, and purified [^{14}C]$NADP^+$ (sp act. 5.35×10^6 cpm/μmol). Malic enzyme was added to a single chamber. $NADP^+$ concentrations were 5–100 μM. The experiments were carried out at 4 °C [(□) 6.7 μM enzyme tetramers], 15 °C [(◇) 14.3 μM enzyme tetramers], and 26 °C [(○) 8.0 μM enzyme tetramers]. Inset: Hill plots of $NADP^+$ binding data.

The Hill coefficient (h) was determined from a Hill plot (Cornish-Bowden, 1976) according to

$$\log \frac{Y}{1-Y} = \log \frac{1}{K_D} + h \log [L]_f \qquad (8)$$

where Y equals the fractional saturation of ligand binding sites, K_D is the dissociation constant of these sites, and h represents the Hill coefficient (index of cooperativity). K_D and h may be calculated from a plot of log $[Y/(1 - Y)]$ against log $[L]_f$.

Where indicated in malate and oxalate binding studies (Figures 5, 6, and 8), the percentage of each initially present, predominant enzyme complex [i.e., E_4–$(Mn^{2+})_2$, E_4–$(Mn^{2+})_4$, etc.; the subscripts indicate the number of ligands bound per tetramer] was obtained from the ratio $[EL]/[E]_t$, with [EL] calculated according to eq 6 and 7, and from known values of $[E]_t$, $[L]_t$, and K_D by using the quadratic equation

$$[EL]^2 - ([E]_t + [L]_t + K_D)[EL] + [L]_t[E]_t = 0 \qquad (9)$$

The following dissociation constants were used for the purpose of these calculations: K_D for the four NADPH sites, 1.1 μM (Table I); K_D for the two tight and two to four weak Mn^{2+} sites, 8 μM and 0.9 mM, respectively (Hsu et al., 1976). In the latter case, the degree of saturation at each of the two types of sites was obtained by a manual reiterative procedure described by Perrin (1965).

The Mn^{2+} concentrations in experiments containing EDTA were corrected for the Mn^{2+}–EDTA complex on the basis of 1:1 equivalency (Welcher, 1958).

Results

Binding of Pyridine Nucleotide Cofactors. Figure 1 shows [^{14}C]$NADP^+$ binding data obtained at pH 7.5 and at several temperatures. The resultant linear Scatchard plots yielded a stoichiometry of 3.70–3.95 binding sites per enzyme tetramer, indicating "all-of-the-sites"[2] binding. The dissociation constant

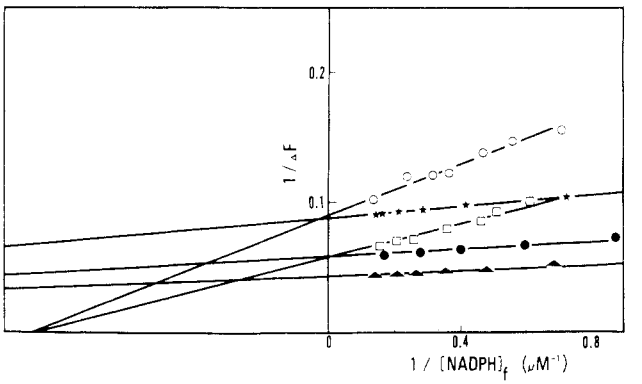

FIGURE 2: Effect of temperature on NADPH binding. The binding of NADPH to malic enzyme was studied by the fluorescence titration technique as described under Methods. The titrations were performed by adding 3-μL aliquots of 0.14 mM NADPH to cuvettes containing enzyme in 50 mM TEA-HCl buffer, pH 7.0, and 1.0 mM DTT, in a total volume of 0.3 mL. The nucleotide fluorescence increments were measured and plotted as $1/\Delta F$ vs. $1/[NADPH]_f$. Filled symbols represent data points from titrations performed at 5 °C: (★) 2.1 μM enzyme tetramers; (●) 3.15 μM enzyme tetramers; (▲) 4.2 μM enzyme tetramers. Open symbols represent data from titrations performed at 30 °C and enzyme concentrations of 2.33 μM (○) and 3.87 μM (□). The fluorescence yield (β') of enzyme-bound NADPH was determined from the limiting initial slope of each F vs. $[NADPH]_t$ plot (not shown) obtained at higher enzyme concentration.

of the binary enzyme–$NADP^+$ complex increased with increasing temperature and was 1.33, 2.21, and 5.94 μM at 4, 15, and 26 °C, respectively. The associated Hill plots yielded a constant slope of 1.00 ± 0.03, indicative of simple hyperbolic binding and equivalence of $NADP^+$ binding sites at the temperatures tested.

The 4.5-fold increase in the dissociation constant, K_D, concurrent with an increase in temperature from 4 to 26 °C was associated with a decrease in the $\Delta G°$ of $NADP^+$ binding from −7.44 to −7.14 kcal/mol. Similar observations were obtained from the binding of NAD^+ to yeast glyceraldehyde-3-phosphate dehydrogenase (Velick et al., 1971; Niekamp et al., 1977).

The temperature dependence of NADPH binding was studied by the fluorescence titration technique. The formation of the binary enzyme–NADPH complex results in a large (3.0–3.45-fold) enhancement (β'/β) of nucleotide fluorescence, which has been used previously to determine the stoichiometry and dissociation constant of NADPH binding at 26 °C (Hsu & Lardy, 1967b). In these studies, titrations were made at 5 and 30 °C by additions of small aliquots of NADPH to cuvettes containing either buffer or enzyme at pH 7.0. Scatchard analyses (not shown) of NADPH titrations gave average values of 3.7 ± 0.3 and 4.1 ± 0.2 NADPH binding sites per enzyme tetramer, respectively, for titrations at 5 and 30 °C. The dissociation constant of NADPH was obtained graphically by the method of Adelstein (1965) from titration values near the equivalence point where the concentrations of both free enzyme and free NADPH are significant. The plots (Figure 2) were linear, and those obtained at each given temperature converged on the X axis, indicating that the NADPH sites are independent and equivalent. The dissociation constant of NADPH was obtained from the negative reciprocal of the X axis intercept and increased with increasing temperature, from a value of 0.29 μM at 5 °C to 1.1 μM at 30 °C. These values are consistent with the previously observed K_D of 0.75 μM at 26 °C (Hsu & Lardy, 1967b) and

[2] The nomenclature was that of Levitzki & Koshland (1976).

Table I: Correlation of Changes in the Dissociation Constant of NADPH and Oxidative Decarboxylase Activity as a Function of Mn^{2+} and Malate Concentrations[a]

expt	[malate] (mM)	[$MnCl_2$] (mM)	ϵ	n	K_D (μM)	V	K_D^0/K_D	V^0/V
1	0.	0	3.00	4.2 ± 0.2	1.1 ± 0.1		0.86	
2	0.1	0.1	6.44	4.1 ± 0.1	0.95 ± 0.1	20.3	1.00	1.0
3	0.1	2.0	4.85	4.2 ± 0.2	1.15 ± 0.2		0.83	
4	0.3	0.1	7.17	4.1 ± 0.1	0.76 ± 0.05	19.4	1.25	1.04
5	1.0	0.1	9.97	4.1 ± 0.1	0.64 ± 0.1	13.8	1.48	1.47
6	5.0	0.1	12.91	4.0 ± 0.1	0.44 ± 0.05	8.9	2.16	2.27
7	5.0	2.0	12.98	4.0 ± 0.1	0.66 ± 0.05	14.1	1.49	1.59
8	15.0	20.0	11.32	4.2 ± 0.2	0.85 ± 0.1			
9	0.5	0.2	7.13	3.7 ± 0.2	0.97 ± 0.1			
10	15.0	0.2	14.61	4.1 ± 0.1	0.36 ± 0.1			

[a] All experiments were performed essentially as described in Figure 2 in 50 mM TEA-HCl buffer and 1 mM DTT, pH 7.0, at 30 °C. The fluorescence titration data were averages of values (±SEM) from two experiments obtained at malic enzyme concentrations of 2.32 and 3.87 μM and the designated substrate concentrations. The rate assays were carried out spectrophotometrically at the same Mn^{2+} and malate concentrations, in the presence of saturating (200 μM) $NADP^+$, at pH 7.0 and 30 °C in the same buffer. n is the stoichiometry of NADPH binding per enzyme tetramer; K_D is the dissociation constant of NADPH; V is the oxidative decarboxylase activity (micromoles of NADPH formed per minute per milligram of enzyme). K_D^0 and V^0 are control values obtained at 0.1 mM each of $MnCl_2$ and malate (experiment 2). ϵ denotes the fluorescence enhancement factor, the ratio of nucleotide fluorescence in E-NADPH or E-Mn^{2+}-NADPH-malate complexes vs. free NADPH. In other experiments (8–10), the dissociation constant of NADPH, at different malate and $MnCl_2$ concentrations, was obtained at constant ionic strength by the addition of KCl to experiments 9 and 10. In addition to the buffer described above, experiments 8–10 also contained 0.1 mM EDTA.

yield $\Delta G°$ values of −8.30 and −8.25 kcal/mol, respectively, at 5 and 30 °C.

The values of $\Delta H_{dissociation}$ for enzyme-bound $NADP^+$ (or NADPH) were calculated from plots of log K_D ($NADP^+$) or log K_D (NADPH) vs. reciprocal absolute temperature and were +11.4 and +8.9 kcal/mol, respectively.

Effect of Substrates on Nucleotide Binding. Previous kinetic results (Hsu et al., 1976) have shown that, at low $MnCl_2$ (<0.1 mM), increasing malate concentration above 0.3 mM inhibited oxidative decarboxylase activity. This inhibition was attributed to the formation of an enzyme–Mn^{2+}–NADPH–malate abortive complex from which NADPH was released more slowly than from the enzyme–NADPH complex (Reynolds et al., 1978b). In this work, further studies were carried out to determine the effects of malate and Mn^{2+} on the dissociation constant of NADPH. Results of the fluorescence titration experiments are shown in Table I. In these experiments, the NADPH binding sites are independent, as indicated by linear Adelstein plots (not shown).

It can be seen in Table I that malate enhanced the fluorescence of enzyme-bound NADPH in the presence of Mn^{2+}, and high Mn^{2+} slightly quenched this fluorescence. The stoichiometry of NADPH obtained by Scatchard analysis (not shown), however, was unchanged, yielding values of 3.7–4.2 binding sites per enzyme tetramer over the entire range of $MnCl_2$ and malate concentrations used. The presence of low levels of $MnCl_2$ and malate (0.1 mM each) had little effect upon the dissociation constant of NADPH. However, the addition of inhibitory levels of malate (0.3–5 mM, experiments 4–6) at this $MnCl_2$ concentration caused progressive decreases in the dissociation constant, up to a factor of 2.2-fold at 5.0 mM malate. An increase in the $MnCl_2$ concentration from 0.1 to 2.0 mM partially offset this decrease (experiment 7). These ligand effects were specific and were observable in experiments corrected for differences in ionic strength (experiments 8–10).

Table I also shows the oxidative decarboxylase activity of malic enzyme obtained at the same $MnCl_2$ and malate concentrations and at saturating $NADP^+$. These results confirm those obtained in previous studies (Reynolds et al., 1978b), that malate at high concentrations (≥0.3 mM) inhibited the catalytic rate in the presence of low $MnCl_2$ (0.1 mM), while higher concentrations of the divalent metal caused deinhibition.

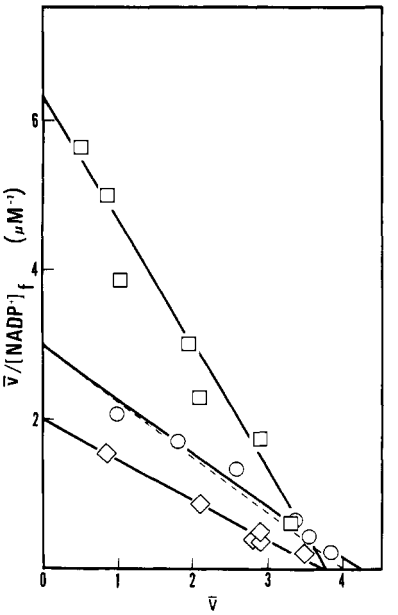

FIGURE 3: Effects of $MnCl_2$ and pyruvate on $NADP^+$ binding. The equilibrium dialysis experiments were performed as indicated in Figure 1 at 4 °C (pH 7.5), except in the presence of indicated levels of $MnCl_2$ and pyruvate: (○) 50 μM $MnCl_2$; (□) 50 μM $MnCl_2$ and 66 mM pyruvate; (◇) 5 mM $MnCl_2$ and 66 mM pyruvate; (- - -) none (plot taken from Figure 1, 4 °C). Malic enzyme concentration: 2–4 μM enzyme tetramers.

There is excellent agreement between the ratios of the dissociation constant of NADPH (K_D^0/K_D) and overall rate (V^0/V) as a function of malate and/or $MnCl_2$, despite large changes in both parameters. This result supports NADPH release as the rate-limiting step (Schimerlik et al., 1977; Reynolds et al., 1978b). Therefore, these changes reflect ligand effects on the "off" constant of this nucleotide.

A study on the effects of $MnCl_2$ and pyruvate upon $NADP^+$ binding was performed by using the technique of equilibrium dialysis. The linear Scatchard plots yielded approximately four (3.75–4.2) equivalent and independent $NADP^+$ binding sites (Figure 3 and Table II), which were unchanged by pyruvate and/or $MnCl_2$. The presence of 50 μM $MnCl_2$ had negligible effect on the dissociation constant of the oxidized nucleotide. This result and our earlier finding that Mn^{2+} ions bind to the

Table II: Effects of Mn^{2+}, Pyruvate, and KCl on $NADP^+$ Binding[a]

additions	n (±0.1)	K_D (μM)
none	3.9	1.3 ± 0.1
$MnCl_2$ (50 μM)	4.2	1.4 ± 0.1
$MnCl_2$ (50 μM); pyruvate (66 mM)	3.75	0.6 ± 0.1
$MnCl_2$ (5 mM); pyruvate (66 mM)	3.75	1.9 ± 0.1
KCl (0.10 M)	4.0	2.9 ± 0.1
KCl (0.20 M)	3.7	2.9 ± 0.1

[a] The experimental data (mean ± SEM) were those obtained from two experiments as shown in Figure 3. The control data (with KCl) were obtained under otherwise identical conditions.

free enzyme (Hsu et al., 1976) are consistent with random binding of $NADP^+$ and Mn^{2+} in the catalytic reaction. Addition of pyruvate (66 mM) in the presence of $MnCl_2$, however, enhanced nucleotide binding 2.2-fold to yield a dissociation constant of 0.6 μM, thus indicating the formation of an enzyme–Mn^{2+}–$NADP^+$–pyruvate abortive complex and tightening of $NADP^+$ binding by pyruvate. An increase in the $MnCl_2$ concentration from 50 μM to 5 mM, in the presence of 66 mM pyruvate, resulted in the increase of the dissociation constant to a value of 1.9 μM for $NADP^+$. The addition of KCl (0.2 M) caused an increase (rather than a decrease) in the dissociation constant of $NADP^+$ from 1.3 to 2.9 μM. Notwithstanding possible specific K^+ and Cl^- effects, this result suggests that the pyruvate-induced tightening of $NADP^+$ binding is not due to increased ionic strength and represents only a minimum estimate.

pH Dependence of Nucleotide Binding. A study on the effect of pH upon the binding of nucleotide coenzymes to an enzyme can give valuable information on the nature of amino acid side chains which contribute to the formation of the binary complex (Knowles, 1976). For this reason and given the availability of methodology, binding experiments of [^{14}C]-$NADP^+$ and NADPH were performed with malic enzyme as a function of pH. In these experiments, the usable pH range was limited by the stability of enzyme and nucleotides and was from pH 6.1 to pH 8.4 for $NADP^+$ and from pH 6.0 to pH 9.2 for NADPH at 4 and 5 °C, respectively.

The pH profiles of the binding parameters of $NADP^+$ and NADPH were obtained from equilibrium dialysis and fluorescence titration studies, respectively. Both nucleotides gave linear Scatchard plots (not shown) at all pH values tested, indicating equivalence of binding sites throughout the pH range employed. Likewise, the binding stoichiometry of four nucleotide sites per enzyme tetramer was independent of pH variation as shown by experimental values (mean ± SD) of 4.01 ± 0.23 (seven determinations) for $NADP^+$, 3.57 ± 0.37 (20 determinations) for NADPH in the binary E–NADPH complex, and 3.78 ± 0.31 (12 determinations) for NADPH binding in the presence of 5 mM malate and 0.1 mM $MnCl_2$. The dissociation constant of $NADP^+$ in the E–$NADP^+$ complex showed no significant variation over pH, with a value of 1.33 ± 0.17 μM (seven determinations).

In the NADPH titration experiments, the NADPH fluorescence was increased by a factor (ϵ; cf. Table I) of ~3.3 (3.15–3.45) in the binary complex and ~6.0 (5.55–6.40) in the E–Mn^{2+}–NADPH–malate quaternary complex. These values were relatively constant up to pH 8.0 for the former and pH 7.4 for the latter; however, both decreased at higher pH values and were 2.43 and 3.05, respectively, at pH 9.2. Adelstein plots were employed for the determination of NADPH dissociation constants. In all cases the plots (not shown) were linear, however, yielding values which were highly

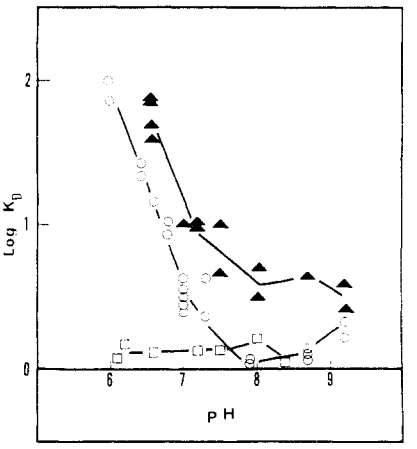

FIGURE 4: Effect of pH on nucleotide binding. $NADP^+$ binding was performed at 4 °C as described in Figure 1 at the pH values indicated by the equilibrium dialysis technique. The dissociation constants (□) were estimated from Scatchard plots. $NADP^+$ was stable at 4 °C for the duration of these experiments (Lowry et al., 1961). NADPH binding was carried out by fluorescence titration experiments at 5 °C as described in Figure 2, at the pH values indicated. The dissociation constants were those obtained in the absence (○) or presence (▲) of 5.0 mM malate and 0.1 mM $MnCl_2$. In these experiments, the absorbancy of NADPH at 340 nm decreased 2.5% at low pH (6.0) and was uncorrected. Malic enzyme was stable in the entire pH range studied.

pH dependent. The dissociation constant of the binary complex increased ~63-fold from an average value of 0.015 μM at pH 6.0 to 0.95 μM at pH 8.0. The addition of 5 mM malate in the presence of 0.1 mM $MnCl_2$, which was inhibitory in the catalytic reaction, did not alter the stoichiometry of binding but enhanced the affinity of NADPH by a factor of ~3 at each pH in the range of 6.6–8.05.

The pH effect on nucleotide binding was further analyzed by the double-log plots shown in Figure 4. Whereas the pH profile of $NADP^+$ binding yielded a flat line indicating a lack of dependency on an ionizable group(s) dissociating in this pH range, the profile for NADPH gave a negative slope of 1.3. This result is consistent with the involvement of one (possibly two) amino acid residue which must be protonated for maximum binding affinity. From the inflection point of the biphasic curve, a pK value of 7.2–7.5 was estimated for this group in the E–NADPH binary complex. The weaker, but relatively constant affinity of NADPH observed at pH values above 8.0 would be expected to result from other interactions between malic enzyme and the nucleotide molecule which are independent of pH or which have pK values which lie outside of the pH studied. It seems likely that malate (in the presence of $MnCl_2$) perturbs these interactions since it induced a ca. threefold enhancement in affinity of NADPH without shifting the pK of the ionizable group.

Binding of L-*Malate.* Malate binding studies were carried out by equilibrium dialysis and fluorescence titration methods in the presence of both the metal and nucleotide cofactors. In these experiments, NADPH (rather than $NADP^+$) was used in order to avoid catalytic turnover. The inclusion of these cofactors tightened the active-site binding of malate, as indicated by previous kinetic and binding studies (Hsu et al., 1967, 1976; Hsu & Lardy, 1967b).

Scatchard plots of [^{14}C]-L-malate binding to ternary enzyme–Mn^{2+}–NADPH complexes, obtained from equilibrium dialysis experiments, are shown in Figure 5. Clearly, these plots are not linear, indicating the presence of heterogeneous malate sites as the result of either preexisting nonidentity or negative cooperativity between initially identical sites. The

Table III: Binding Parameters of Malate[a]

expt	$[Mn^{2+}]$ (mM)	equilibrium dialysis				fluorescence titration	
		N_1	K_1 (μM)	N_2	K_2 (μM)	K_1 (μM)	K_2 (μM)
1	0.1[b]	1.7 ± 0.1	22 ± 3	2.1 ± 0.1	350 ± 36	30 ± 4	250 ± 36
2	9.9[b]	2.1 ± 0.1	23 ± 3	2.0 ± 0.1	400 ± 36		
		(1.9)[c]	(31)[c]	(2.0)[c]	(400)[c]		

[a] The parameters shown for equilibrium dialysis experiments were those used to fit the smooth curves in Figure 5. The parameters from fluorescence titrations were obtained as described in the text and Figure 7. The values are mean ± SEM (two experiments). [b] Corrected for the Mn^{2+}-EDTA complex. [c] The parameters in parentheses were those used to fit Scatchard plots which used free malate concentrations corrected for the Mn^{2+}-malate complex (K_D = 20 mM; Hsu et al., 1976).

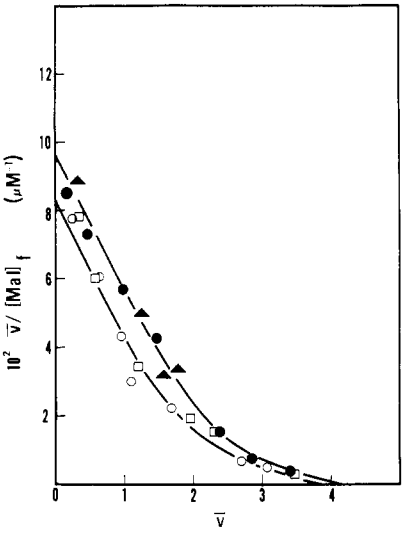

FIGURE 5: Equilibrium binding of [^{14}C]-L-malate to ternary complexes. The malate binding studies were performed at 4 °C by the equilibrium dialysis technique as described under Methods. Both chambers of each dialysis cell contained 50 mM TEA-HCl, pH 7.0, 0.1 mM EDTA, 1.0 mM DTT, saturating (0.21 mM) NADPH, and amounts of purified [^{14}C]-L-malate (sp act. 11.8 × 10^6 cpm/μmol) and $MnCl_2$ as indicated. Malic enzyme (26–52 μM tetramers) was added to a single chamber. Experiment 1: 0.2 mM $MnCl_2$ (open symbols); malate concentrations, 9 μM–0.6 mM. Experiment 2: 10 mM $MnCl_2$ (filled symbols); malate concentrations, 16 μM–1.8 mM. The ionic strength of reaction mixtures in experiment 1 was brought to the level of experiment 2 with KCl (30 mM). Each experiment was carried out in duplicate as shown by the different symbols. Under these experimental conditions, the NADPH sites were 98% saturated. After correction for chelation of Mn^{2+} by EDTA (cf. Methods), the predominant ternary enzyme complexes were, experiment 1, 83% E_4–$(Mn^{2+})_2$–$(NADPH)_4$ and, experiment 2, 92% E_4–$(Mn^{2+})_{4-6}$–$(NADPH)_4$. The points were experimental observations, and the smooth curves were drawn by reiterative fitting to eq 6, assuming four sites with two types of affinity.

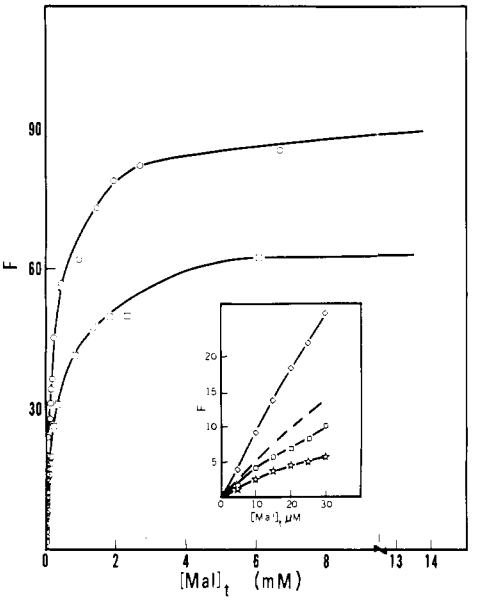

FIGURE 6: Effect of malate on the nucleotide fluorescence of ternary malic enzyme complexes. The fluorescence titration experiments were carried out as described under Methods by the addition of small aliquots of malate to cuvettes containing saturating (0.21 mM) NADPH, 0.2 mM $MnCl_2$, and malic enzyme in 50 mM TEA-HCl buffer, 0.1 mM EDTA, and 1 mM DTT in a total volume of 0.2 mL. The nucleotide fluorescence intensity was followed after initially adjusting the instrument reading to zero prior to malate addition. The malic enzyme concentrations were (□) 4.15 and (○) 6.23 μM tetramers. The predominant ternary enzyme complex was E_4–$(Mn^{2+})_2$–$(NADPH)_4$, 83%. Neither $MnCl_2$ nor malate alone affected the fluorescence of free NADPH. Inset: enlarged view of the above plot at low malate concentrations and additional plots obtained at enzyme concentrations of (☆) 2.08 and (◇) 16.6 μM.

parameters used to fit the smooth curves are given in Table III. The values obtained for E–Mn^{2+}–$(NADPH)_4$ complexes, with Mn^{2+} (0.1 mM after correcting for the Mn^{2+}–EDTA complex) occupying only tight or Mn^{2+} (9.9 mM) occupying both tight and weak metal sites, were not significantly different and were consistent with the presence of two sets of malate sites per enzyme tetramer, each set containing two (1.7–2.1) sites with the same affinity for malate. The dissociation constants for the tight and weak sites were 22 to 23 μM and 350–400 μM, respectively.

At high $MnCl_2$ concentration (9.9 mM, experiment 2), a significant amount of the Mn^{2+}–malate complex was formed. However, the binding parameters (Table III, values in parentheses) obtained after correcting for complexed malate were not significantly altered.

Control malate binding experiments were performed in the absence of either $MnCl_2$, NADPH (with 10 mM total $MnCl_2$), or both or in the presence of $NADP^+$ alone (260 μM), under otherwise identical conditions. In all cases horizontal Scatchard plots (i.e., slope ≃ 0) were obtained, yielding weak affinity malate sites with dissociation constants in the millimolar (>2 mM) range. Thus, both Mn^{2+} and nucleotide are required to promote malate binding. The large uncertainty in experimental points due to weak binding precluded an accurate estimation of the binding stoichiometry. However, no significant change in this parameter was seen, as indicated by the binding of four to five malate molecules by the E_4–$(Mn^{2+})_4$ complex (at 10 mM total $MnCl_2$) at a malate concentration of 5.8 mM.

The presence of heterogeneous malate sites with differing affinities was also confirmed by fluorescence titration experiments in which fluorescence increments were monitored upon the addition of malate to a malic enzyme solution containing NADPH and $MnCl_2$. The large enhancement of nucleotide fluorescence of the E–Mn^{2+}–NADPH complex by malate has been reported previously (Hsu & Lardy, 1967b) and was demonstrated in the present work (Table I). The titration curves of E_4–$(Mn^{2+})_2$–$(NADPH)_4$ at several levels of malic enzyme are shown in Figure 6. In these experiments, malate

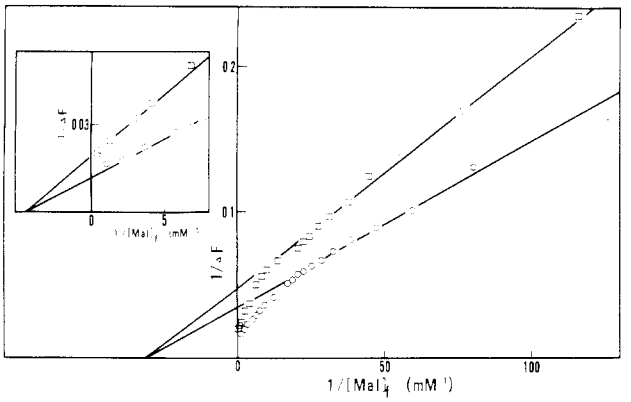

FIGURE 7: Adelstein plots of malate binding. The data points were obtained from the experiment shown in Figure 6. The free malate concentration ($[Mal]_f$) was calculated according to $[Mal]_f = [Mal]_t - [E\text{–}Mal]$ with a β' value of 3.0, calculated from Figure 6 as described under Methods. Inset: an enlarged plot at high malate concentrations.

Table IV: Parameters of Oxalate Binding to Malic Enzyme[a]

additions	K_{EO} (μM)	n
none	65 ± 3.5	2.0 ± 0.1
$MnCl_2$ (60 μM)	53 ± 3.5	1.9 ± 0.1
$MnCl_2$ (10 mM)[b]	78 ± 7	2.0 ± 0.1
NADPH (200 μM)	17 ± 1.4	2.0 ± 0.1
$MnCl_2$ (75 μM); NADPH (200 μM)[b]	20 ± 2.1	2.1 ± 0.1
$MnCl_2$ (75 μM); NADPH (200 μM); malate (500 μM)	249 ± 57[c]	2.2 ± 0.1

[a] The results (mean ± SEM, two experiments) were obtained as shown in Figure 8. K_{EO} and n are, respectively, the dissociation constant and stoichiometry of oxalate. [b] The predominant enzyme complexes were as follows: 10 mM $MnCl_2$, 92% E_4–$(Mn^{2+})_4$; 75 μM $MnCl_2$ and 200 μM NADPH, 81% E_4–$(Mn^{2+})_2$–$NADPH_4$. [c] The apparent K_{EO} was determined from the Scatchard plot according to the modified Scatchard equation $\bar{\nu}/[O]_f = (1/K_{EO,app})(n - \bar{\nu})$ where $K_{EO,app} = K_{EO}(1 + [M]_f/K_{EM})$, assuming competitive binding of malate and oxalate.

did not affect the fluorescence of enzyme bound NADPH in the absence of $MnCl_2$, as would be expected if the metal ion was required for malate binding. A fluorescence yield (β') of 3.0 arbitrary fluorescence units/μM bound malate was obtained. It should be noted that this value represents the result of malate binding at the tight substrate sites (see below). If we assume that it is unchanged upon binding at the weak sites, the total binding stoichiometry may be calculated from the maximum fluorescence (Figure 6, at 14 mM malate), obtained at three enzyme concentrations, to yield an average of 5.3 ± 1.7 malate sites per enzyme tetramer. Despite the large uncertainty, this stoichiometry is consistent with the presence of four malate sites. Significantly, both Scatchard (not shown) and Adelstein (Figure 7) plots of these data were biphasic, indicating nonequivalency of binding sites with dissociation constants of 30 ± 4 μM and 250 ± 36 μM (Figure 7 and Table III). Meaningful values for the stoichiometry of each type of binding site, however, could not be obtained. The good agreement of dissociation constants from fluorescence titrations with those obtained by equilibrium dialysis experiments indicates that NADPH fluorescence increases in proportion to the fractional saturation of total malate sites irrespective of a change in binding affinity.

Binding of [^{14}C]*Oxalate.* The binding of oxalate, which has previously been shown as a potent inhibitor of pyruvate in the reductase and reductive carboxylation reactions (Hsu et al., 1976), was performed by the equilibrium dialysis technique using [^{14}C]oxalate. The results of these experiments are shown as Scatchard plots in Figure 8 and the calculated binding

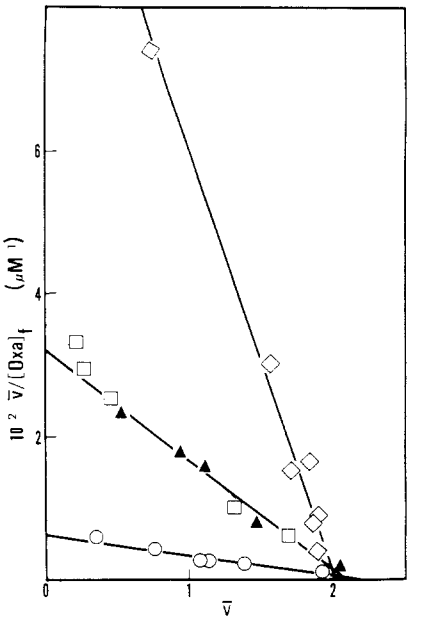

FIGURE 8: Equilibrium binding of oxalate to malic enzyme. The oxalate binding studies were performed at 4 °C by the equilibrium dialysis technique as described under Methods. Both chambers of each dialysis cell contained 50 mM TEA-HCl buffer, pH 7.0, 1 mM DTT, purified [^{14}C]oxalate (sp act. 6.4 × 10^6 cpm/μmol), and other ligands as indicated. Malic enzyme (4–9 μM tetramers) was added to a single chamber. The oxalate concentrations were 10 μM–1.4 mM. The additions were (▲) none, (◇) NADPH [200 μM, 99.8% E_4–$(NADPH)_4$], (□) (dashed line) $MnCl_2$ [60 μM, 81% E_4–$(Mn^{2+})_2$], and (○) $MnCl_2$ (75 μM), NADPH (200 μM), and malate (500 μM).

parameters are summarized in Table IV. Oxalate binds malic enzyme tightly with a stoichiometry of two sites per enzyme tetramer, indicating half-of-the-sites[2] reactivity. The binding stoichiometry was unchanged by the presence of reactants such as Mn^{2+}, NADPH, or malate, singly or in combination. The affinity of oxalate for the unliganded enzyme (K_D = 65 μM) and its binary complexes [E_4–$(Mn^{2+})_2$; E_4–$(NADPH)_4$] obtained in these studies were similar to those obtained previously by the PRR technique (Hsu et al., 1976) and showed a 3.5-fold tightening of oxalate binding (K_D = 17–20 μM) by saturation with NADPH. In contrast to malate, however, oxalate binding was not enhanced by the binding of Mn^{2+} at the tight metal sites (K_D = 53 μM at 60 μM $MnCl_2$) or both tight and weak metal sites (K_D = 78 μM at 10 mM $MnCl_2$). The former is identical with a value of 52 μM obtained by PRR titrations.

Table IV also shows that malate decreased the affinity of oxalate for the ternary E_4–$(Mn^{2+})_2$–$(NADPH)_4$ complex. If oxalate (O) binds at the substrate site in direct competition with malate (M), the dissociation constant of malate (K_{EM}) may be calculated from K_{EO} (20 μM) and apparent K_{EO} (349 μM) according to

$$K_{EM} = \frac{K_{EO}[M]_f}{K_{EO,app} - K_{EO}} \qquad (10)$$

Under these experimental conditions (0.5 mM malate), the fraction of bound malate was very small. Therefore, the free malate concentration was nearly equal to the total malate concentration. Substitution of $[M]_t$ for $[M]_f$ into eq 10 yielded a malate dissociation constant of 30 μM for the E–Mn^{2+}–NADPH–malate complex. This value is in good agreement with the value of 22–30 μM found for the tight malate sites by direct binding studies (Table III), thereby providing experimental support for the binding of oxalate at the active site.

Covalent Modification Studies. Previous chemical modification studies with the affinity label bromopyruvate have

Table V: Reaction of Chemically Modified Malic Enzyme with KCN[a]

incubn time (h)	E_4(S-TNB)$_4$[b] no. of $^{14}CN^-$/ tetramer	sp act. (units/mg)	E_4(S-pyr)$_2$(S-TNB)$_2$[b] no. of $^{14}CN^-$/ tetramer	sp act. (units/mg)
0		<0.4		<4.0
0.7	0.40		0.18	
2.0	1.25		0.60	
4.2	2.25		1.15	
6.7	3.20		1.50	
10.0	3.40		1.70	
16.7	3.45 (3.5)[c]	36	1.70 (1.6)[c]	<4.0

[a] Malic enzyme derivatives were prepared from the fully active (40 units/mg of protein), NEM-premodified enzyme $E_4(SH)_4$, containing 4.04 SH groups per tetramer, by further modification with either DTNB (reaction 14) or sequential modification with bromopyruvate followed by DTNB (reactions 11 and 12) according to Pry & Hsu (1978, Figure 2). The DTNB-modified enzyme E_4(S-TNB)$_4$ was <1% active, containing no detectable SH groups. The bromopyruvate-modified enzyme E_4(S-pyr)$_2(SH)_2$ was <10% active and contained 2.27 SH groups per tetramer. The bromopyruvate-DTNB sequentially modified enzyme E_4(S-pyr)$_2$(S-TNB)$_2$ was <10% active and contained no detectable SH groups. The chemically modified derivatives were treated with $K^{14}CN$ (4.5 mM; 1.6×10^4 cpm/μmol) (reactions 13 and 15) in 50 mM Tris-HCl buffer, pH 7.0, at 0 °C. Aliquots were taken at the designated time intervals and analyzed for malic enzyme activity, protein-bound radioactivity, and thionitrobenzoate (TNB) release at 412 nm with an extinction coefficient of 13 600 M^{-1} cm^{-1} (Tang & Hsu, 1974). The reactions are

$$E_4(SH)_4 + \text{bromopyruvate} \rightarrow E_4(\text{S-pyr})_2(SH)_2 \quad (11)$$

$$E_4(\text{S-pyr})_2(SH)_2 + \text{DTNB} \rightarrow E_4(\text{S-pyr})_2(\text{S-TNB})_2 \quad (12)$$

$$E_4(\text{S-pyr})_2(\text{S-TNB})_2 + K^{14}CN \rightarrow E_4(\text{S-pyr})_2(S\text{-}^{14}CN)_2 + \text{TNB} \quad (13)$$

$$E_4(SH)_4 + \text{DTNB} \rightarrow E_4(\text{S-TNB})_4 \quad (14)$$

$$E_4(\text{S-TNB})_4 + K^{14}CN \rightarrow E_4(S\text{-}^{14}CN)_4 + \text{TNB} \quad (15)$$

[b] The stoichiometry of thionitrobenzoate incorporation was confirmed by titration with 5 mM dithiothreitol, yielding 4.05 molecules of free TNB per tetramer for E_4(S-TNB)$_4$ and 109% recovery of activity and 1.94 molecules of free TNB per tetramer for E_4(S-pyr)$_2$(S-TNB)$_2$ with no increase in activity. [c] Numbers in parentheses indicate the number of TNB released per tetramer after reaction with KCN.

demonstrated that it reacts with only two SH groups out of the four available, thereby yielding half-of-the-sites stoichiometry (Chang & Hsu, 1977a). This behavior is further indicated by the experiment shown in Table V. In this experiment, the active enzyme and the bromopyruvate-inactivated enzyme, containing two modified SH groups, were treated with DTNB to affect alkylation. The covalently attached TNB groups were then cleaved with $K^{14}CN$. The extent of ^{14}C incorporation and the extent of TNB release agree well with each other and confirm the expected stoichiometry of these enzyme derivatives. The complete regeneration of activity by the $E_4(S\text{-}^{14}CN)_4$ enzyme establishes the noncatalytic nature of these SH groups.

Discussion

The present results on $NADP^+$ and NADPH binding indicate the presence of one nucleotide site on each of the putatively identical subunits of the tetrameric malic enzyme molecule (Nevaldine et al., 1974). These nucleotide sites are equivalent and independent. The dissociation constants of both nucleotides, obtained under conditions comparable to those in activity assays (pH 7–7.5; 26–30 °C), are in the range of those calculated from previous kinetic studies (Hsu et al., 1967; Schimerlik & Cleland, 1977a), indicating the detection of catalytically competent sites. The all-of-the-sites stoichiometry

Scheme I: Mechanism for the pH Dependence of NADPH Binding[a]

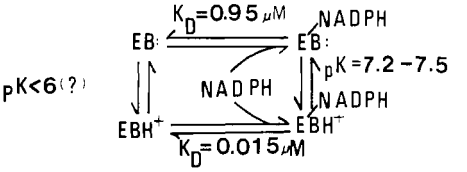

[a] E denotes malic enzyme and B: is the deprotonated imidazole side chain of histidine. The dissociation constant of EB:–NADPH is the average value at pH 8.0, whereas that of EBH–NADPH is the average value at pH 6.0 where 94% of the group is in the protonated form, assuming a pK of 7.2.

and equivalency are unchanged over the wide range of pH and temperatures tested (Figures 1 and 2 and cf. pH Dependence of Nucleotide Binding), nor are these parameters affected by the presence of Mn^{2+} and/or the nonreacting carboxylic acid substrates (i.e., pyruvate for $NADP^+$ binding and malate for NADPH binding; Figure 4 and Tables I and II). The increased affinity of both nucleotides with decreasing temperature (Figures 1 and 2) suggests that polar forces rather than hydrophobic forces play a major role in the binding of these coenzymes with this dehydrogenase (Scheraga, 1963).

The binding of $NADP^+$ for malic enzyme was found to be independent of pH in the range of 6.1–8.4 (Figure 4), indicating that this process did not involve a group(s) ionizing in the above pH range. The same conclusion was drawn by Schimerlik & Cleland (1977b) from a kinetic study on the pH profile of $\bar{V}/K$ for $NADP^+$. The latter study showed a dependence of $NADP^+$ binding on the ionization of a group with pK of 5.3 and the protonation of a group with a pK of 9.3. Attempts made by us to identify these groups by direct binding studies were unsuccessful, however, due to the instability of both malic enzyme and $NADP^+$ during the longer time period required for equilibrium dialysis experiments at these extreme pH values.

In contrast, the binding affinity of NADPH was highly pH dependent (Figure 4) and decreased ~63-fold from pH 6.0 to pH 8.0 owing to the ionization of one (or two) group with a pK of 7.2–7.5. This value does not correspond to those of NADPH (i.e., pK of 3.9 and 6.1; Dawson et al., 1969). Therefore, it is assigned to the ionization of a neutral amino acid(s) on the enzyme such as histidine (Cohn & Edsall, 1943). The value for the $\Delta H_{\text{dissociation}}$ of E–NADPH of 8.9 kcal/mol agrees with the known value of 6.9–7.5 kcal/mol for the heat of ionization of an imidazole group (Dixon & Webb, 1964). This analysis is consistent with results of our previous chemical modification studies (Chang & Hsu, 1977a), which showed that the histidine reagent ethoxyformic anhydride abolished the ability of this enzyme to bind nucleotide cofactors.

A simple mechanism for the pH dependence of NADPH binding is shown in Scheme I.

A protonated histidyl group has been implicated in the binding of NADH by several NAD^+-linked dehydrogenases such as yeast alcohol dehydrogenase (Dickenson & Dickinson, 1977), pig heart malate dehydrogenase, and lactate dehydrogenase (Lodola et al., 1978), and it was suggested that this group functions as a proton sink in the lactate dehydrogenase reaction (Winer & Schwert, 1958; Dalziel, 1963). Our results are compatible with such a role for the histidyl residue of malic enzyme. It seems likely that the high affinity of NADPH at lower pH results from interactions between the dihydronicotinamide ring of the nucleotide and the protonated histidine residue at (or near) the binding site, in a manner analogous to the NAD^+-linked enzymes. The lower, but relatively constant affinity of NADPH at higher pH values

Scheme II: Quaternary Complexes of Malic Enzyme[a]

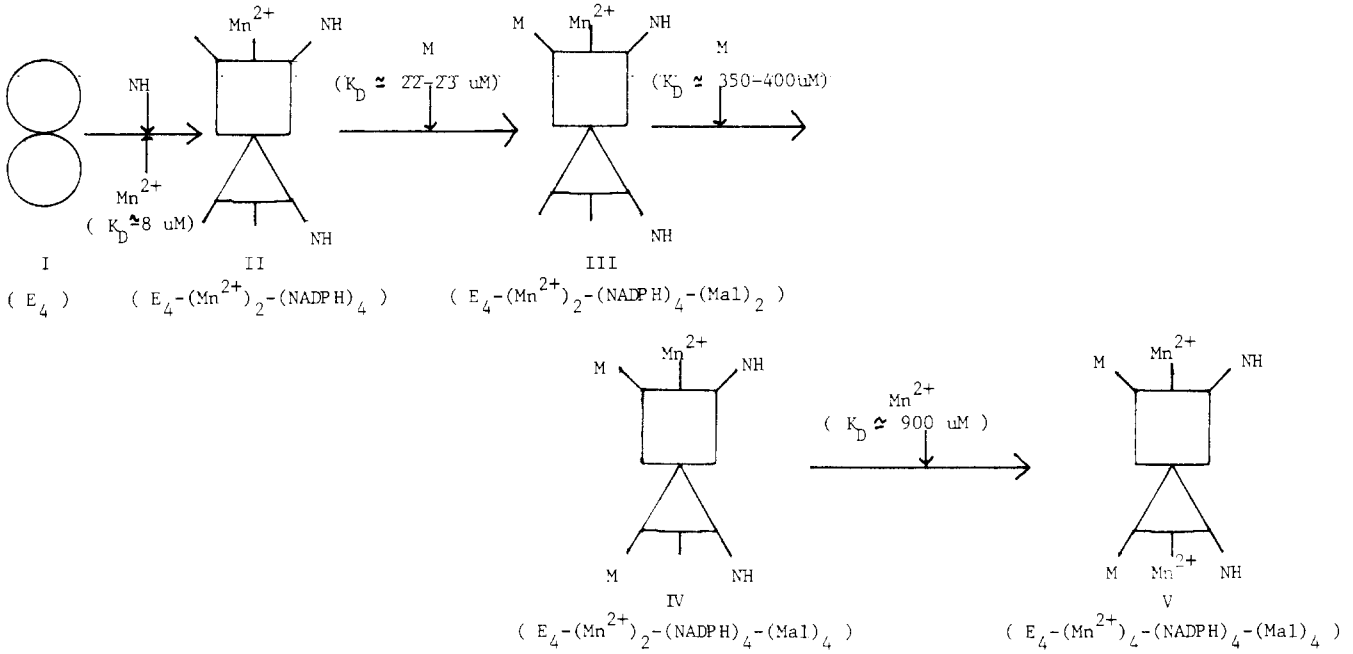

[a] NH and M denote NADPH and malate, respectively. The enzyme complex representing each tetramer is abbreviated in parentheses. Subunits of the unliganded enzyme (circles in I) are initially identical, as judged by their molecular size (Nevaldine et al., 1974), by the reactivity of SH groups, and by their nucleotide binding behavior.

(pH >8.0) may be attributed to interactions with hydrophobic and/or basic amino acid residues. The dissociation constant of $\simeq 0.95$ μM at this pH is quantitatively similar to the pH-independent K_D of 1.33 μM for $NADP^+$ (cf. Binding of Pyridine Nucleotide Cofactors), suggesting the involvement of these interactions in the binding of both nucleotides. Furthermore, the ca. threefold increase in NADPH affinity by malate (Figure 4) may be explained by an enhancement of these interactions.

Since $NADP^+$ binding is not pH dependent in the range of pH 6.1–8.4, its impairment upon reversible ethoxyformylation of histidyl residues (Chang & Hsu, 1977a) appears to be due to a steric effect caused by the presence of the bulky ethoxyformyl group.

Nucleotide binding properties of several $NADP^+$-linked dehydrogenases, such as glucose-6-phosphate dehydrogenase (Levy, 1979), phosphogluconate dehydrogenase (Silverberg & Dalziel, 1975), glutamate dehydrogenase (Dalziel & Egan, 1972), and isocitrate dehydrogenase (Ehrlich & Colman, 1975; Reynolds et al., 1978a) have been previously reported. However, to the best of our knowledge, this is the first detailed analysis on the pH dependence of nucleotide binding by such an enzyme using direct equilibrium methods.

While the nucleotide coenzymes exhibit all-of-the-sites reactivity with equivalent and noninteracting sites, the binding behavior of carboxylic acid reactants is more complex, showing anticooperativity or possibly heterogeneous binding sites due to preexisting asymmetry. Strong evidence for the former was obtained in chemical modification experiments with the affinity label bromopyruvate, which has the unique property of being either a substrate (under catalytic conditions with cofactors present) or a covalent modifier of the enzyme, reacting with only two SH groups out of the four available (Chang & Hsu, 1977a,b). This half-of-the-sites behavior is confirmed by the results of the KCN experiment (Table V) in the current work. In contrast, all-of-the-sites stoichiometry of reaction is shown by nonspecific reagents such as iodoacetate, iodoacetamide, DTNB, and NEM (Pry & Hsu, 1978), attesting to the equivalency of SH groups. The existence of ligand-induced negative cooperativity rather than preexisting heterogeneity in binding sites was more clearly demonstrated for the bromopyruvate-modified enzyme $E_4(S\text{-pyr})_2(SH)_2$ by our observation that the two unmodified SH groups of this enzyme reacted with DTNB and NEM more slowly than did the SH groups of the fully active enzyme $E_4(SH)_4$ (Pry & Hsu, 1978).

Half-of-the-sites stoichiometry of binding was observed with oxalate, the isoelectronic analogue of the enolate of pyruvate (Figure 8 and Table IV). The active-site binding of oxalate was demonstrated by the competitive inhibition of this process by malate occupying tight substrate sites. The high affinity of oxalate in the binary E_4–$(Oxa)_2$ and ternary E_4–$(Mn^{2+})_2$–$(Oxa)_2$ complexes and its enhancement by NADPH generally confirm results of earlier PRR studies (Hsu et al., 1976). The large increase ($\sim$600-fold) in affinity over pyruvate (K_D = 36 mM) is also in keeping with the postulated role of oxalate as a transition-state analogue. A similar function was assigned to this compound in the reaction of biotin carboxylases using pyruvate as the substrate (Fung et al., 1974; Mildvan et al., 1966; Northrop & Wood, 1969). The lack of a significant Mn^{2+} effect upon oxalate binding is unexpected. Since Mn^{2+} tightens malate binding (Figure 5; cf. Binding of L-Malate), this result might suggest that Mn^{2+} functions to lower the barrier for the formation of the transition-state complex with malate.

The ability of malic enzyme to form binary complexes with Mn^{2+} (Hsu et al., 1976) or $NADP^+$ (Figure 1) suggests a random order of addition for these cofactors in the oxidative decarboxylation reaction. Since $NADP^+$ binds before malate in the sequential mechanism (Hsu et al., 1967) and Mn^{2+} (together with NADPH) promotes specific malate binding (see Binding of L-Malate), it may be concluded that malate binds last in the reaction following both Mn^{2+} and $NADP^+$. The uncompetitive substrate inhibition vs. [Mn^{2+}] [Figure 2 in Hsu & Pry (1980)] is consistent with this binding order.

Studies on the malate binding parameters of the E–Mn^{2+}–NADPH complex, with Mn^{2+} occupying the two tight

or both tight and weak metal sites, yielded a stoichiometry of four malates per enzyme tetramer. As with Mn^{2+}, two of these sites bind malate tightly, while the remainder are weak sites more than 1 order of magnitude lower in affinity. These results confirm and extend our previous analysis (Hsu et al., 1976) of two sets of malate sites on the enzyme. The affinity of malate for enzyme complexes without Mn^{2+} or NADPH or both is considerably weaker but the binding remains specific, as indicated by the essentially unchanged stoichiometry of substrate sites. Since the enzyme also contains four nucleotide sites and four to six metal sites, it follows that each subunit of the tetrameric molecule has a "complete" active site, capable of specific binding of all reactants of the reaction. While it is conceivable that the biphasic binding of Mn^{2+} and malate could be accounted for by the presence of equal amounts of two isozymes with differing affinities, such an explanation seems very unlikely from a number of considerations. Two malic enzyme bands have been detected in our preparations by activity staining after disc gel electrophoresis (Liu and Hsu, unpublished results). However, the major band comprised at least 85% of the total protein.

The formation of various E–Mn^{2+}–NADPH–malate complexes and plausible interactions between subunits accounting for the nonequivalency in binding behavior are demonstrated in Scheme II for a single dimer in a dimer-of-dimers structure. This scheme incorporates the independent association of NADPH as well as the anticooperative behavior of Mn^{2+} and malate, each of which binds sequentially to tight (square) and weak (triangle) sites as a function of concentration. NADPH and Mn^{2+} bind randomly to the free enzyme. Occupancy of Mn^{2+} at the tight sites in complex II (with NADPH on all sites) promotes tight malate binding on the same sites to yield complex III or both tight and weak malate binding to yield complex IV. Occupancy of Mn^{2+} at the weak sites then yields the fully liganded complex V. Thus, while tight binding of Mn^{2+} and malate is ordered (i.e., Mn^{2+} first), weak binding of these reactants is random as shown in an alternative sequence with complex VI rather than complex IV as the intermediate. The ability of tightly bound Mn^{2+} to affect malate binding at neighboring Mn^{2+}-deficient subunits (complex IV) provides strong evidential support for the existence of a "ligand-induced" interaction between these subunits.

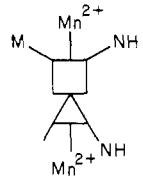

complex VI, E_4-$(Mn^{2+})_4$-$(NADPH)_4$-$(Mal)_2$

In the following paper, steady-state kinetic experiments are performed to determine the functional significance of these two types of heterogeneous enzyme sites.

Acknowledgments

The authors are indebted to Dr. W. W. Cleland at the Biochemistry Department, University of Wisconsin, Madison, WI, and Dr. Albert S. Mildvan at the Institute for Cancer Research, Philadelphia, PA, for reviewing the manuscript and offering constructive suggestions on the interpretation of some of our results before publication.

References

Adelstein, S. J. (1965) *Biochemistry 4*, 891–896.

Chang, G. G., & Hsu, R. Y. (1977a) *Biochemistry 16*, 311–320.

Chang, G. G., & Hsu, R. Y. (1977b) *Biochim. Biophys. Acta 483*, 228–235.

Cohn, E. J., & Edsall, J. T. (1943) *Proteins, Amino Acids, and Peptides*, p 445, Reinhold, New York.

Cornish-Bowden, A. (1976) *Principles of Enzyme Kinetics*, pp 120–122, Butterworths, Boston, MA.

Dalziel, K. (1963) *J. Biol. Chem. 238*, 2850–2858.

Dalziel, K., & Egan, R. R. (1972) *Biochem. J. 126*, 975–984.

Dawson, R. M. C., Elliott, D. C., Elliott, W. H., & Jones, K. M. (1969) *Data for Biochemical Research*, p 204, Oxford University Press, New York.

Dickenson, C. J., & Dickinson, F. M. (1977) *Biochem. J. 161*, 73–82.

Dixon, M., & Webb, E. C. (1964) *Enzymes*, p 144, Academic Press, New York.

Edsall, J. T., & Wyman, J. (1958) *Biophysical Chemistry*, Vol. 1, p 613, Academic Press, New York.

Ehrlich, R. S., & Colman, R. F. (1975) *Biochemistry 14*, 5008–5016.

Fromm, H. J. (1963) *J. Biol. Chem. 238*, 2938–2944.

Fung, C. H., Mildvan, A. S., & Leigh, J. S. (1974) *Biochemistry 13*, 1160–1169.

Hsu, R. Y., & Lardy, H. A. (1967a) *J. Biol. Chem. 242*, 520–526.

Hsu, R. Y., & Lardy, H. A. (1967b) *J. Biol. Chem. 242*, 527–532.

Hsu, R. Y., & Pry, T. A. (1980) *Biochemistry* (following paper in this issue).

Hsu, R. Y., Lardy, H. A., & Cleland, W. W. (1967) *J. Biol. Chem. 242*, 5315–5322.

Hsu, R. Y., Mildvan, A. S., Chang, G. G., & Fung, C. H. (1976) *J. Biol. Chem. 251*, 6574–6583.

Knowles, J. R. (1976) *CRC Crit. Rev. Biochem. 4*, 165–173.

Levitzki, A., & Koshland, D. E., Jr. (1976) *Curr. Top. Cell. Regul. 10*, 1–40.

Levy, H. R. (1979) *Adv. Enzymol. Relat. Areas Mol. Biol. 48*, 98–192.

Lewis, K. F., & Weinhouse, S. (1957) *Methods Enzymol. 3*, 269–276.

Lodola, A., Parker, D. M., Jeck, R., & Holbrook, J. J. (1978) *Biochem. J. 173*, 597–605.

Lowry, O. H., Passonneau, J. V., & Rock, M. K. (1961) *J. Biol. Chem. 236*, 2756–2759.

Mildvan, A. S., Scrutton, M. C., & Utter, M. F. (1966) *J. Biol. Chem. 241*, 3488–3498.

Nevaldine, B. H., Bassel, A. R., & Hsu, R. Y. (1974) *Biochim. Biophys. Acta 336*, 283–293.

Niekamp, C. W., Sturtevant, J. M., & Velick, S. F. (1977) *Biochemistry 16*, 436–445.

Northrup, D. B., & Wood, H. G. (1969) *J. Biol. Chem. 244*, 5801–5807.

Owens, H. S., Goodban, A. E., & Stark, J. B. (1953) *Anal. Chem. 25*, 1507–1511.

Perrin, D. D. (1965) *Nature (London) 206*, 170–171.

Pry, T. A. (1979) *Abstracts for 11th International Congress of Biochemistry*, p 286.

Pry, T. A., & Hsu, R. Y. (1978) *Biochemistry 17*, 4024–4029.

Reynolds, C. H., Kuchel, P. W., & Dalziel, K. (1978a) *Biochem. J. 171*, 733–742.

Reynolds, C. H., Hsu, R. Y., Matthews, B., Pry, T. A., & Dalziel, K. (1978b) *Arch. Biochem. Biophys. 189*, 309–316.

Scatchard, G. (1949) *Ann. N.Y. Acad. Sci. 51*, 660–672.

Scheraga, H. A. (1963) *Proteins, 2nd Ed. 1*, 545-546.
Schimerlik, M. I., & Cleland, W. W. (1977a) *Biochemistry 16*, 565-570.
Schimerlik, M. I., & Cleland, W. W. (1977b) *Biochemistry 16*, 576-583.
Schimerlik, M. I., Grimshaw, C. E., & Cleland, W. W. (1977) *Biochemistry 16*, 571-576.
Silverberg, M., & Dalziel, K. (1975) *Methods Enzymol. 41*, 214-220.
Tang, C. L., & Hsu, R. Y. (1974) *J. Biol. Chem. 249*, 3916-3922.
Tomkins, G. M., Yielding, K. L., & Curran, J. F. (1962) *J. Biol. Chem. 237*, 1704-1708.
Velick, S. F., Baggott, J. P., & Sturtevant, J. M. (1971) *Biochemistry 10*, 779-786.
Weder, H. G., Schildnecht, J., Lutz, R. A., & Kesselring, P. (1974) *Eur. J. Biochem. 42*, 475-481.
Welcher, F. J. (1958) *Analytical Uses of Ethylenediaminetetraacetic Acid*, pp 1-17, Van Nostrand, New York.
Winer, A. D. (1964) *J. Biol. Chem. 239*, 3598-3600.
Winer, A. D., Schwert, G. W., & Miller, D. B. S. (1959) *J. Biol. Chem. 234*, 1149-1154.

Kinetic Studies of the Malic Enzyme of Pigeon Liver. "Half-of-the-Sites" Behavior of the Enzyme Tetramer in Catalysis and Substrate Inhibition†

Robert Y. Hsu* and Terry A. Pry‡

ABSTRACT: A steady-state analysis is carried out at pH 7.0 to determine the kinetic significance of the two types of Mn^{2+} and malate binding sites on malic enzyme, detectable by direct binding studies [Pry, T. A., & Hsu, R. Y. (1980) *Biochemistry* (preceding paper in this issue)]. At saturating $NADP^+$, malate exhibits Michaelis-Menten behavior, with K_A (Mn^{2+}) of 8.5-33 μM and K_M (malate) of 47-63 μM, corresponding to the binding of these reactants at two "tight" metal [$K_D \simeq 8$ μM; Hsu, R. Y., Mildvan, A. S., Chang, G. G., & Fung, C. H. (1976) *J. Biol. Chem. 251*, 6574-6583] and substrate ($K_D \simeq 23$-30 μM) sites. Saturation of Mn^{2+} at "weak" metal sites ($K_D \simeq 0.9$ mM) has no effect on the catalytic rate. High (but physiological) levels of malate cause uncompetitive substrate inhibition vs. [Mn^{2+}], at low Mn^{2+} concentrations occupying only the tight metal sites. The apparent K_i of malate is 182-270 μM, which corresponds to the binding of malate at two remaining weak sites ($K_D \simeq 250$-400 μM). High concentrations of Mn^{2+} relieve malate inhibition with a K_A' of $\simeq 0.64$ mM, as the result of binding at weak metal sites. A "half-of-the-sites" model is proposed which shows that only two of the four putatively identical subunits of this enzyme simultaneously undergo catalysis. The catalytic rate is inhibited by malate through binding at the adjacent low-affinity sites, and the inhibition is overcome by binding of Mn^{2+} at the same sites. Malate also inhibits the Mg^{2+}-activated reaction. Under in vivo conditions, malic enzyme probably exists in the partially inhibited form, subject to regulation by changes in the levels of malate and the metal activator.

Previous EPR studies (Hsu et al., 1976) have shown that malic enzyme of pigeon liver binds the activating metal Mn^{2+} at two high-affinity sites and two to four low-affinity sites. In the preceding paper of this series, we reported equilibrium binding studies on $NADP^+$, NADPH, the substrate malate, and the inhibitor oxalate. The nucleotides bind independently and equivalently to the putatively identical subunits of the enzyme tetramer. Malate binding is promoted by Mn^{2+} and NADPH in accordance with an ordered kinetic mechanism with malate binding last in the reaction sequence. As with Mn^{2+}, malate binds to two types of sites with differing affinity. "Half-of-the-sites" reactivity is shown by the inhibitor oxalate which binds firmly to only two of the available sites. Mn^{2+} shows kinetic negative cooperativity at inhibitory levels of malate, and the double-reciprocal velocity vs. [Mn^{2+}] plots concave downward with increasing Mn^{2+} concentration. This paper presents a more detailed steady-state kinetic study using $NADP^+$ concentration saturating the four available sites and Mn^{2+} and malate concentrations saturating the two high-affinity sites or both high- and low-affinity sites. The unusual kinetic and binding behavior of this enzyme uncovered in these studies is interpreted in terms of a half-of-the-sites model whereby only two of the four enzyme sites are simultaneously undergoing catalysis. A preliminary report of this work has been published (Hsu & Pry, 1979).

Experimental Section

Materials

TEA-HCl (A grade),[1] EDTA, Tris-HCl (enzyme grade), and DTT (Calbiochem), L-malic acid (Schwarz/Mann), $NADP^+$ (P-L Biochemicals), Sephadex G-200 (Pharmacia), Dowex 1-X10 (Mallinckrodt), DE-52 (Whatman), and $MnCl_2$ (Fischer Scientific) were purchased from the above sources. Distilled, deionized water was used throughout this work. The nucleotide solutions were made up fresh daily.

Methods

The preparation of pigeon liver malic enzyme and enzyme assays were performed as described in the preceding paper (Pry & Hsu, 1980). One unit of enzyme activity is defined as the amount which catalyzes the conversion of 1 μmol of substrate per min under the conditions of the assay. The kinetic assays

† From the Department of Biochemistry, State University of New York, Upstate Medical Center, Syracuse, New York 13210. *Received August 9, 1979.* Supported in part by grants from the National Institutes of Health (AM 13390 and 5507RR05402). This research is derived from the dissertation of T.A.P. presented in partial fulfillment for the requirements of a Ph.D. degree.

‡ Present address: Lipid Metabolism Laboratory, Veteran's Administration Hospital, Madison, WI 53705.

[1] Abbreviations used: TEA-HCl, triethanolamine hydrochloride; Tris, tris(hydroxymethyl)aminomethane; DTT, dithiothreitol.

0006-2960/80/0419-0962$01.00/0